Microwave multimode memory with an erbium spin ensemble

S. Probst,[1] H. Rotzinger,[1] A. V. Ustinov,[1] and P. A. Bushev[2,*]

[1]*Physikalisches Institut, Karlsruhe Institute of Technology, D-76128 Karlsruhe, Germany*
[2]*Experimentalphysik, Universität des Saarlandes, D-66123 Saarbrücken, Germany*

Hybrid quantum systems combining circuit QED with spin-doped solids are an attractive platform for distributed quantum information processing. There, the magnetic ions serve as coherent memory elements and reversible conversion elements of microwave to optical qubits. Among many possible spin-doped solids, erbium ions offer the unique opportunity for a coherent conversion of microwave photons into the telecom C band at 1.54 μm employed for long distance communication. In our work, we perform a time-resolved electron spin resonance study of an $Er^{3+} : Y_2SiO_5$ spin ensemble at millidegrees Kelvin temperatures and demonstrate multimode storage and retrieval of up to 16 coherent microwave pulses. The memory efficiency is measured to be 10^{-4} at a coherence time of $T_2 = 5.6$ μs. We observe a saturation of the spin coherence time below 50 mK due to full polarization of the surrounding electronic spin bath.

PACS number(s): 03.67.Hk, 42.50.Pq, 76.30.Kg

I. INTRODUCTION

Future quantum communication technology will combine three basic types of subsystems: transmission channels, repeater stations, and information processing nodes [1,2]. Similarly to classical communication networks, photons propagating through optical fiber channels are ideal for carrying quantum states over long distances and distributing entanglement between information processing nodes [3]. These computational nodes or quantum processors may be realized by employing single atomic or macroscopic solid-state systems. Among a plethora of solid-state devices, superconducting (SC) qubits are one of the most promising building blocks for a future quantum computer [4]. Many groundbreaking experiments have been recently demonstrated with SC qubits, including the measurement of long coherence and relaxation times of up to 0.1 ms [5], coherent operation of up to three-qubit processors [6], the implementation of a deterministic two-qubit gate [7], and the realization of a basic surface code for fault tolerant computing [8]. These qubits operate at microwave frequencies and cryogenic temperatures. In order to embed them into the emerging quantum optical internet technology, a coherent interface between optical and microwave photons is required [9].

Ensembles of rare-earth (RE) ions doped into a crystal are a suitable system for coherent photon conversion between optical and microwave frequency bands [10–12]. Such RE-doped crystals are currently at the forefront of quantum communication research, where many thrilling achievements such as the demonstration of a quantum memory at the optical telecom C band around 1.54 μm [13], high efficiency storage of optical photons [14], generation of entanglement between two RE-doped crystals [15], and quantum teleportation between a telecom O-band photon (1.34 μm) and a RE-doped crystal [16] have been reported. Also, RE-doped crystals are considered to have a great potential as a multimode optical memory element in future quantum repeater technology [17], and the storage and retrieval of 64 temporal optical modes at the single photon level has been demonstrated [18].

A crucial step towards the development of a microwave to optical interface requires highly efficient reversible mapping of temporal microwave modes into the rare-earth spin ensemble at a power level corresponding to a single microwave photon [19]. In that respect, circuit quantum electrodynamics (QED) experiments with RE-doped crystals contributed a first step towards the implementation of a quantum memory [20,21]. The strong coupling regime accompanied by large collective coupling strengths of 30–200 MHz has been recently demonstrated [22–24]. However, reversible mapping of temporal microwave modes in a RE spin ensemble has yet to be shown. So far, most of the time-resolved microwave experiments with RE-doped crystals have been limited to investigations of their coherence and magnetic properties performed in conventional electron spin resonance (ESR) spectrometers at temperatures above 2 K [25–28].

In this paper, we investigate the spin coherence properties of an $Er^{3+} : Y_2SiO_5$ (Er:YSO) crystal at millidegrees Kelvin temperatures and demonstrate the successful storage and on-demand retrieval of 16 weak coherent microwave pulses. Such a crystal is known for the longest measured optical coherence time of about 4.4 ms among solid-state systems at a telecom wavelength around 1.54 μm [29]. Thus, the Er:YSO crystal is considered as a promising candidate for reversible coherent conversion of microwave photons into the optical telecom C band [10,11].

II. EXPERIMENTAL SETUP

Figure 1(a) shows a picture of the experimental setup. We investigate a single Er:YSO crystal (Scientific Materials, Inc.) doped with 0.005% atomic concentration of Er^{3+} ions and with dimensions of $3 \times 4 \times 5$ mm. The inset of this figure presents the orientation of the crystal axes D_1, D_2, b with respect to the applied dc magnetic field B. The crystal orientation ($\theta \simeq 45°$) maximizes the coupling strength for the high-field transition S_{2a} [22]. The crystal is placed on top of a coplanar waveguide $\lambda/2$ microwave resonator fabricated on a high-frequency laminate (Rogers TMM 10i). In contrast to our previous investigations [20,22,23], a nonsuperconducting copper resonator is employed. Such a resonator does not perturb the magnetic dc field, therefore, we expect to attain

---
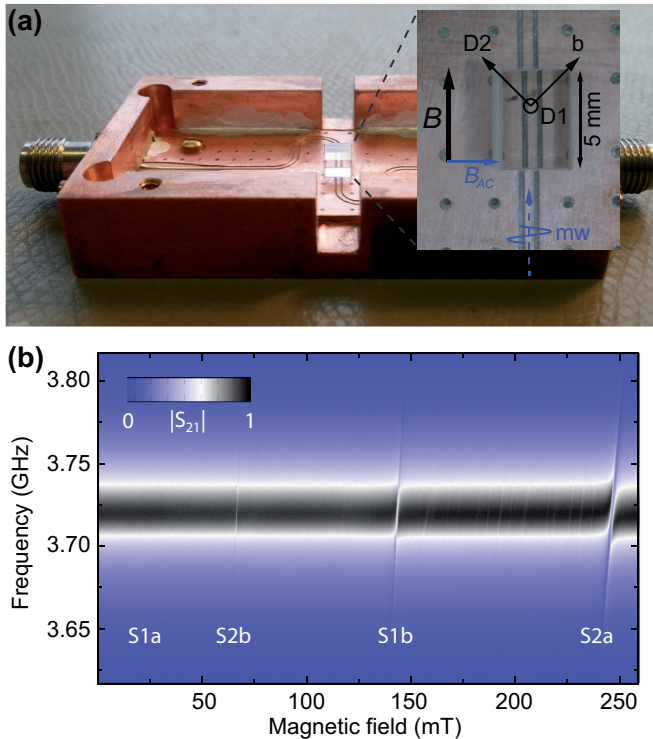
FIG. 1. (Color online) (a) Experimental setup: The Er:YSO crystal is placed on a $\lambda/2$ copper coplanar waveguide resonator. Inset: Orientation of the crystal with respect to the dc magnetic field B. In this experimental configuration, the oscillating magnetic field $B_{ac}(\omega)$ is perpendicular to B. (b) Transmission ESR spectrum of Er:YSO coupled to the resonator. The color code on the right-hand side illustrates the magnitude of the microwave amplitude transmission coefficient $|S_{21}(\omega)|$ through the chip.

a minimally inhomogeneous spin linewidth of the erbium spin ensemble. The width of the coplanar waveguide is about 0.5 mm with gaps of about 0.25 mm. The comparably large geometric dimensions of the resonator are beneficial for optical access and for attaining an intrinsic quality factor of $Q_i \simeq 400$. The experiment is placed inside a copper housing and cooled by a BlueFors LD-250 dilution fridge to 25 mK. For further details on the experimental setup, we refer to Ref. [30].

III. MICROWAVE SPECTROSCOPY AND HAHN ECHO DETECTION

Initially, the sample is characterized in the common way by continuous wave (cw) microwave transmission spectroscopy while sweeping the magnetic field [31,32]. Figure 1(b) presents the resulting spectrum recorded at 25 mK and a probing power of $\sim$100 fW. The transmitted amplitude is color coded and all four subensembles with g factors 14.2, 4.0, 1.9, and 1.1 are resolved. The electronic transition close to 140 mT shows a weak anticrossing, indicating the onset of strong coupling. A clear normal mode splitting is observed for the high-field transition S_{2a} at a magnetic field of 246 mT.

In this paper, we focus our analysis on the high-field transition S_{2a} at 246 mT with $g = 1.1$. The avoided level
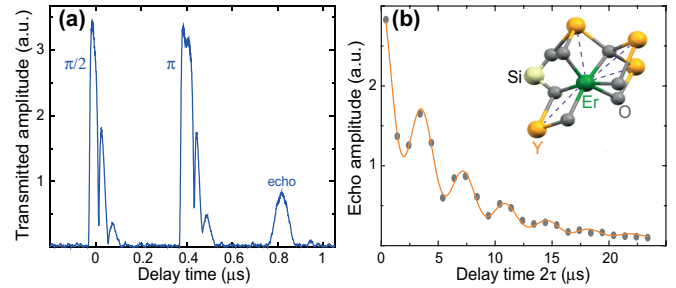
FIG. 2. (Color online) (a) Hahn echo sequence with a pulse separation of $\tau = 400$ ns. Each pulse is accompanied by vacuum Rabi oscillations. The $\pi/2$ pulse has a width of 20 ns. The spin echo appears as a 100 ns wide pulse due to the finite bandwidth of the resonator. (b) The echo decay is modulated by prominent oscillations, which are known as electron spin-echo envelope modulation (ESEEM). This originates from the coupling of the erbium electronic spins to the nuclear spins of the neighboring ^{89}Y ions. The solid line presents a fit to the data, yielding $T_2 \simeq 5.6$ μs.

crossing is analyzed by first fitting the resonator far away from the transition. This yields a resonance frequency of $\omega_0/2\pi = 3.721$ GHz and a half width at half maximum (HWHM) linewidth of $\kappa/2\pi = 8.2 \pm 0.1$ MHz. By using these parameters, we extract a collective coupling strength of $v_N/2\pi = 13.2 \pm 0.7$ MHz and a HWHM inhomogeneous spin linewidth of $\Gamma_2^\star/2\pi = 7.3 \pm 0.4$ MHz.

On the basis of the cw spectroscopy, we performed time-resolved ESR experiments in the temperature range 0.02–1 K. Due to the large mode volume of the resonator compared to the previous experiments with SC resonators [20,22,23], strong microwave pulses (1–10 mW) are necessary for coherent spin manipulation. Therefore, no additional cryogenic attenuation was used in the experiment (see Ref. [30] for details). Thus, we estimate the number of thermal photons in the cavity to be about $n_{ph} \sim 50$. For comparison, the number of spins coupled to a resonator mode is $N_s \sim 3 \times 10^{13} \gg n_{ph}$, therefore, the thermal photons do not significantly affect the polarization of the spin ensemble.

Figure 2(a) shows a two-pulse Hahn echo (2PE) sequence $\pi/2$-τ-π followed by an echo emission. The length of the π pulse is set to be 40 ns and its magnitude is about 10 mW. The free induction decay is not observable here because the large inhomogeneous broadening results in a very short pure dephasing time $T_2^* \simeq 22$ ns. The shape of the transmitted $\pi/2$ and π pulses reveals a cavity decay during $\sim$100 ns modulated by vacuum Rabi oscillations. Thus, a short but strong pulse does not affect the Tavis-Cummings dynamics of the hybrid system.

Figure 2(b) presents the amplitude of the echo signal in dependence on the total delay time 2τ. The oscillatory modulation of the echo decay is attributed to electron spin-echo envelope modulation (ESEEM) [33], which originates from the dipole-dipole coupling of the erbium electronic spin to nuclear spins in close proximity [34]. The closest magnetic dipoles are the nuclear spins of the yttrium ^{89}Y ions with magnetic moment $\mu_Y = -0.275\mu_N$ at an average distance of $\sim$4 Å. The fit to the modulated exponential decay yields a spin coherence time of $T_2 = 5.6$ μs.

IV. TEMPERATURE DEPENDENCE OF SPIN COHERENCE TIME

In the following, we study the decoherence mechanisms of the erbium spin ensemble S_{2a}. There are two major contributions to decoherence: (I) dephasing induced by the surrounding magnetic environment, i.e., other electronic or nuclear spins [35], and (II) direct spin-spin interaction within the same spin ensemble [36]. Source (I) is addressed by investigating the temperature dependence of the coherence time T_2. The increase of the coherence time due to the "freezing" of the surrounding spin bath has been observed in mm-wave ESR with paramagnetic materials [35,37]. Those experiments were performed above 2 K, requiring a magnetic field of several tesla to ensure full polarization of the electronic spin bath. In contrast, the base temperature of our experiment (25 mK) entails operation at the GHz frequency range while maintaining full polarization at only ~100 mT [see also Fig. 1(b)].

Figure 3 presents the temperature dependence of Er:YSO spin coherence time T_2 from 30 mK to 1 K. In the displayed temperature range, the T_2 time increases by approximately 1 μs. Below 50 mK, T_2 remains constant, indicating that magnetic fluctuations are "frozen out" [35]. Since the spin-lattice relaxation time is measured to be ~10 s in the experimental temperature range (see, for example, Refs. [22,38] for the measurement technique), it does not limit T_2.

In order to account for the observed behavior of T_2, we have to consider the influence of the other three erbium spin subensembles in the YSO crystal, which create a surrounding electronic spin bath. The spin concentration of each ensemble is $n_s \simeq 10^{17}$ cm^{-3} and their g factors vary from 1.9 to 14.2. These ensembles present a considerable
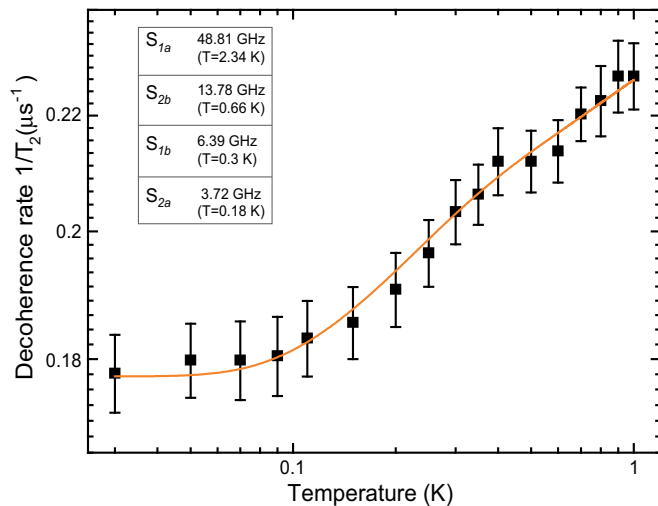
FIG. 3. (Color online) Temperature dependence of the decoherence rate $1/T_2$ of the S_{2a} ensemble measured by the spin-echo experiment. Note the semilogarithmic scale. Between 30 mK and 1 K, the T_2 time decreases from approximately 5.6 to 4.4 μs. The solid line is a fit to theory [see Eq. (1)], which takes into account thermal fluctuations from the surrounding erbium subensembles. Inset: Transition frequencies and effective temperatures at magnetic field of $B = 246$ mT of all subensembles.

fluctuating magnetic background. To put the Zeeman transition frequencies into perspective, Fig. 3 also provides the effective Zeeman temperatures of each subensemble $T_i = g_i \mu_B B / k_B$, where k_B is the Boltzmann constant. As the temperature rises, the background spins perform random flip flops, altering the precession frequencies of the S_{2a} ensemble [39]. The occupation probabilities are given by the Boltzmann statistics, $P_\uparrow = [1 + \exp(T_i/T)]^{-1}$ and $P_\downarrow = [1 + \exp(-T_i/T)]^{-1}$. By including a residual dephasing rate Γ_r, the temperature dependence of T_2 is described by [35,37]

$$\frac{1}{T_2(T)} = \Gamma_r + \sum_{i=1}^{3} \frac{\xi}{(1 + e^{T_i/T})(1 + e^{-T_i/T})}, \qquad (1)$$

where ξ is a temperature-independent free parameter given by the dipole-dipole interaction strength [40].

The solid line in Fig. 3 presents a fit of Eq. (1) to the data, where Γ_r and ξ are the only free parameters. Below 100 mK, the temperature dependence saturates and the fit yields $\Gamma_r = (5.63 \ \mu s)^{-1}$. Also, the fit reproduces the data, including the slightly shallower slope towards larger temperatures. Thus, the spin flip-flop processes of the other three subensembles dominate the temperature dependence of coherence time T_2.

The suppression of optical decoherence of site 1 of Er:YSO due to an increase in magnetic order has also been reported in Ref. [40]. There, instead of lowering the temperature, one can increase the magnetic field to values of about 3–5 T at in the temperature range of 1.6–4 K. Similar investigations employing 0.005% Er:YSO report an optical coherence time ranging from 10 to 70 μs depending on the orientation of the crystal in the magnetic field [29].

We now turn to the analysis of the sources of the residual decoherence rate at low temperatures. The second source of decoherence are spin flip-flop processes within the same subensemble. These give rise to instantaneous spin diffusion, which cannot be refocused by a standard 2PE sequence. However, it is possible to measure this dipolar interaction with a modified 2PE sequence where the angle of the second pulse θ_2 is varied from 0 to π [41]. The π angle corresponds to a standard 2PE sequence and refocuses the magnetic field inhomogeneity and low frequency magnetic noise. If a spin flip flop occurs, the θ_2 pulse cannot refocus this interaction because the pulse flips both spins involved in the interaction as they belong to the same spin ensemble. The longest coherence time measured by applying the $\pi/2$-τ-θ_2 sequence is $T_2 = 7 \ \mu$s. From the dependence $T_2(\theta_2)$ we infer a dipole-dipole coupling strength between neighboring spins in S_{2a} of $\nu_D/2\pi = 12$ kHz.

Further contributions to the residual decoherence rate Γ_r are the fluctuating yttrium nuclear spin bath and the ^{167}Er isotope with nuclear spin 7/2 and 22% natural abundance. However, with the present setup we are not able to differentiate between those contributions. To conclude this section, the electronic spin bath given by the other spin sub ensembles does not impact the coherence at the lowest temperature in the present setting. The residual decoherence rate can be lowered by diluting the spin ensemble, i.e., by reducing the dipole-dipole coupling, and removing the ^{167}Er isotope by isotopic purification.

V. MULTIMODE COHERENT MEMORY

Next, we demonstrate a microwave multimode memory with Er^{3+} : Y_2SiO_5 by storing and retrieving 16 weak coherent pulses. In a multimode spin ensemble quantum memory, an incoming photon is mapped onto a coherent spin wave of the ensemble [42]. A single photon being absorbed by an ensemble of N spins manifests itself as a coherent superposition of all possibilities of one spin being excited with the rest in the ground state. In an inhomogeneously broadened ensemble, one has to consider the different precession frequencies of the spins, yielding

$$|\Psi\rangle_{\text{ph}} = \frac{1}{\sqrt{N}} \sum_{k=1}^{N} |\downarrow_1 \downarrow_2 \cdots \uparrow_k \cdots \downarrow_N\rangle e^{-i\delta_k t}, \qquad (2)$$

where δ_k denotes the detuning of the kth spin from the mean precession frequency of the ensemble. As the time t progresses, this state dephases into a dark mode, such that the bright mode can absorb the next photon. A desired but feasible quantum memory would be able to store multiple photons. In a spin ensemble, the number of stored modes is limited by $N_m = T_2/T_2^*$. However, in our experiment, the finite bandwidth of the resonator stretches the echo emission to about 100 ns, reducing the number of effective modes to approximately 56. Upon application of a π pulse, the time evolution is reversed and all the dark modes rephase again, emitting a photon. Thus, the time order of the incident photons is reversed with respect to the sequence of emitted photons.
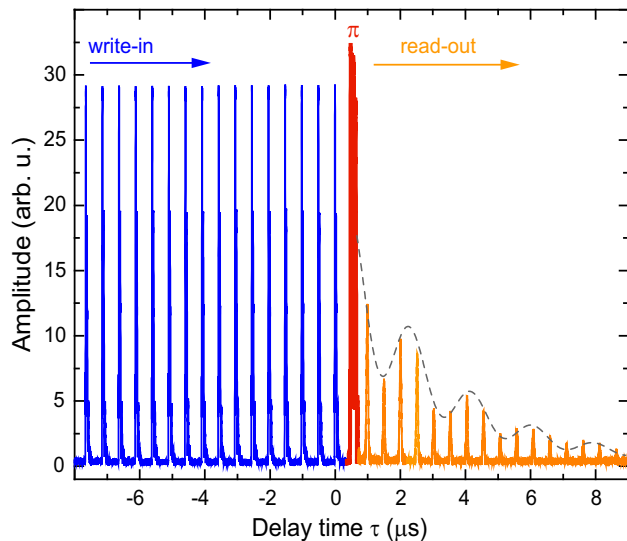
FIG. 4. (Color online) Storage of 16 microwave coherent pulses in the S_{2a} erbium spin ensemble. All input pulses are of the same height and 10 ns width. The amplitudes of the refocusing and input pulses are in the saturation limit of our amplifiers and appear smaller in the plot. The retrieved pulse stream shown in the plot is exponentially damped and exhibits oscillatory behavior due to the coupling of the electronic spins to the nuclear spins of ^{89}Y ions (ESEEM). The dotted curve is identical to the ESEEM signal presented in Fig. 2(b). The ESEEM signal is superimposed in the present graph to demonstrate the oscillating envelope of the readout pulses.

Figure 4 presents the complete sequence of writing in and reading out of 16 microwave coherent pulses. For the pulse preparation and detection we employ a heterodyne setup. The probing sequence is prepared by using upconversion of pulses at $\omega_s/2\pi = 200$ MHz to the resonance frequency $\omega_0/2\pi = 3.721$ GHz (see Ref. [30] for details). Every incoming pulse contains about $\sim 4.6 \times 10^{11}$ photons and corresponds to a power level of 115 μW.

The transmitted microwave signal is amplified, filtered, downconverted back to $\omega_s/2\pi = 200$ MHz, and digitized by a personal computer (PC). The signal is averaged 595 times with a repetition rate of 10 mHz. Such a low repetition rate is necessary to repolarize electronic spins into their thermal equilibrium. As expected, the amplitude of the readout (emitted) pulse train decays towards longer storage times, and the decay pattern shows modulations attributed to ESEEM. Since we employ a heterodyne detection scheme, we are insensitive to incoherent emission. Thus, the readout pulse train detected in our experiment has a fixed (coherent) phase relation to the write-in signal.

The performance of a memory is defined by the efficiency for a pulse being stored during the coherence time T_2 (5.6 μs for the present system) of the spin ensemble. In order to determine the memory efficiency, the pulse energy at T_2 after the refocusing pulse is analyzed and compared to the energy of the input pulse. Note, the energy of the input pulses was determined in a separate calibration procedure. We obtain an energy retrieval efficiency of 10^{-4} at T_2.

VI. DISCUSSION

Storage of microwaves in the high power regime ($n_{\text{ph}} \sim 10^{14}$) has been reported, by using a conventional ESR spectrometer [43]. The memory efficiency in that experiment was 10^{-10}. An investigation by Grezes *et al.* [44] demonstrates storage and retrieval of extremely weak microwave pulses ($n_{\text{ph}} \sim 3$ photons) in a nitrogen vacancy spin ensemble with an efficiency of 2×10^{-4} at a temperature of 300 mK. In their experiment, the spin dephasing limits the efficiency of the memory. In this paper the main limitation comes from the inhomogeneity of the ac field. The magnitude of the ac field, and therefore the Rabi frequency, decreases inversely proportional to the distance between a spin and the resonator. Consequently, the refocusing pulse is only effective for a very small subset of spins with the appropriate Rabi frequency. This may be improved by the application of optimal control pulse schemes [45] and cleverer resonator designs with very homogeneous ac fields [46] in conjunction with surface spin-doped samples [38].

Quite recently, Grezes *et al.* succeeded in improving their experiment, and they demonstrate storage of coherent microwave pulses at the single photon level with an improved efficiency of 0.3% at a temperature of 100 mK [47]. The two key improvements were an enhanced active reset scheme at 100 mK combined with an isotopically purified sample reducing decoherence originating from the ^{13}C spin bath.

Ultimately, RE-ion-doped crystals with better coherence properties are required. For instance, crystals predominantly doped with RE isotopes with nonzero nuclear spin (^{167}Er or ^{143}Nd) features $T_2 \simeq 100$ μs [25,28], while maintaining

sufficient optical depth [48]. Even longer coherence times of the hyperfine transitions are attained by operating the microwave memory at a *clock transition* [49,50], where the spin's precession frequency is to first order insensitive to magnetic field fluctuations. Alternatively, one can transfer microwave excitations from the electronic to the nuclear spins of the rare-earth ions [51].

VII. CONCLUSIONS

In conclusion, we have presented a detailed pulsed ESR study of an Er:YSO crystal at millidegrees Kelvin temperatures. The coherence time of the spin ensemble at millidegrees Kelvin temperature is measured to be about 5.6 μs, which allowed us to store and retrieve up to 16 weak coherent pulses. The clear ESEEM signal originating from the coupling of the erbium spins to ^{89}Y nuclear spins holds a great potential

of employing them as a nuclear spin quantum memory. The moderate increase of the coherence time below 1 K suggests that the electronic spin bath given by the other spin subensembles does not limit the spin coherence in the present experiment. The presented work paves the way towards applying rare-earth doped crystals as a reversible conversion element between microwaves and telecom C-band photons at 1.54 μm.

[1] D. P. DiVincenzo, Fortschr. Phys. **48**, 771 (2000).

[2] N. Gisin and R. Thew, Nat. Photonics **1**, 165 (2007).

[3] T. E. Northup and R. Blatt, Nat. Photonics **8**, 356 (2014).

[4] M. H. Devoret and R. J. Schoelkopf, Science **339**, 1169 (2013).

[5] H. Paik, D. Schuster, L. S. Bishopa, G. Kirchmair, G. Catelani, A. Sears, B. Johnson, M. Reagor, L. Frunzio, L. Glazman *et al.*, Phys. Rev. Lett. **107**, 240501 (2011).

[6] M. D. Reed, L. DiCarlo, S. E. Nigg, L. Sun, L. Frunzio, S. M. Girvin, and R. Schoelkopf, Nature (London) **482**, 382 (2012).

[7] L. Steffen, Y. Salathe, M. Oppliger, P. Kurpiers, M. Baur, C. Lang, C. Eichler, G. Puebla-Hellmann, A. Fedorov, and A. Wallraff, Nature (London) **500**, 319 (2013).

[8] R. Barends, J. Kelly, A. Megrant, A. Veitia, D. Sank, E. Jeffrey, T. C. White, J. Mutus, A. G. Fowler, B. Campbell *et al.*, Nature (London) **508**, 500 (2014).

[9] L. Tian, P. Rabl, R. Blatt, and P. Zoller, Phys. Rev. Lett. **92**, 247902 (2004).

[10] C. O'Brien, N. Lauk, S. Blum, G. Morigi, and M. Fleischhauer, Phys. Rev. Lett. **113**, 063603 (2014).

[11] L. A. Williamson, Y.-H. Chen, and J. J. Longdell, Phys. Rev. Lett. **113**, 203601 (2014).

[12] K. Xia and J. Twamley, Phys. Rev. A **91**, 042307 (2015).

[13] B. Lauritzen, J. Minar, H. de Riedmatten, M. Afzelius, N. Sangouard, C. Simon, and N. Gisin, Phys. Rev. Lett. **104**, 080502 (2010).

[14] M. P. Hedges, J. J. Longdell, Y. Li, and M. J. Sellars, Nature (London) **465**, 1052 (2010).

[15] I. Usmani, C. Clausen, F. Bussière, N. Sangouard, M. Afzelius, and N. Gisin, Nat. Photonics **6**, 234 (2012).

[16] F. Bussières, C. Clausen, A. Tiranov, B. Korzh, V. B. Verma, S. W. Nam, F. Marsili, A. Ferrier, P. Goldner, H. Herrmann *et al.*, Nat. Photonics **8**, 775 (2014).

[17] C. Simon, H. de Riedmatten, M. Afzelius, N. Sangouard, H. Zbinden, and N. Gisin, Phys. Rev. Lett. **98**, 190503 (2007).

[18] I. Usmani, M. Afzelius, H. de Riedmatten, and N. Gisin, Nat. Commun. **1**, 12 (2010).

[19] M. Afzelius, N. Sangouard, G. Johansson, M. U. Staudt, and C. M. Wilson, New J. Phys. **15**, 065008 (2013).

[20] P. Bushev, A. K. Feofanov, H. Rotzinger, I. Protopopov, J. H. Cole, C. M. Wilson, G. Fischer, A. Lukashenko, and A. V. Ustinov, Phys. Rev. B **84**, 060501(R) (2011).

[21] M. Staudt, I. Hoi, P. Krantz, M. Sandberg, M. Simoen, P. Bushev, N. Sangouard, M. Afzelius, V. Shumeiko, G. Johansson *et al.*, J. Phys. B **45**, 124019 (2012).

[22] S. Probst, H. Rotzinger, S. Wünsch, P. Jung, M. Jerger, M. Siegel, A. Ustinov, and P. A. Bushev, Phys. Rev. Lett. **110**, 157001 (2013).

[23] A. Tkalčec, S. Probst, D. Rieger, H. Rotzinger, S. Wünsch, N. Kukharchyk, A. D. Wieck, M. Siegel, A. V. Ustinov, and P. Bushev, Phys. Rev. B **90**, 075112 (2014).

[24] W. Farr, M. Goryachev, J. le Floch, P. Bushev, and M. Tobar, arXiv:1412.0086.

[25] S. Bertaina, S. Gambarelli, A. Tkachuk, I. N. Kurkin, B. Malkin, A. Stepanov, and B. Barbara, Nat. Nanotechnol. **2**, 39 (2007).

[26] S. Bertaina, J. H. Shim, S. Gambarelli, B. Z. Malkin, and B. Barbara, Phys. Rev. Lett. **103**, 226402 (2009).

[27] R. M. Rakhmatullin, I. N. Kurkin, G. V. Mamin, S. B. Orlinskii, M. R. Gafurov, E. I. Baibekov, B. Z. Malkin, S. Gambarelli, S. Bertaina, and B. Barbara, Phys. Rev. B **79**, 172408 (2009).

[28] E. I. Baibekov, M. R. Gafurov, D. G. Zverev, I. N. Kurkin, B. Z. Malkin, and B. Barbara, Phys. Rev. B **90**, 174402 (2014).

[29] T. Böttger, C. W. Thiel, R. L. Cone, and Y. Sun, Phys. Rev. B **79**, 115104 (2009).

[30] S. Probst, Ph.D. thesis, Karlsruhe Institute of Technology, 2015, Karlsruhe, http://digbib.ubka.uni-karlsruhe.de/volltexte/1000045286.

[31] D. Schuster, A. Sears, E. Ginossar, L. DiCarlo, L. Frunzio, J. Morton, H. Wu, G. Briggs, B. Buckley, D. Awschalom *et al.*, Phys. Rev. Lett. **105**, 140501 (2010).

[32] W. G. Farr, D. L. Creedon, M. Goryachev, K. Benmessai, and M. E. Tobar, Phys. Rev. B **88**, 224426 (2013).

[33] A. Schweiger and G. Jeschke, *Principles of Pulse Electron Paramagnetic Resonance* (Oxford University Press, New York, 2001).

[34] O. Guillot-Noël, H. Vezin, P. Goldner, F. Beaudoux, J. Vincent, J. Lejay, and I. Lorgeré, Phys. Rev. B **76**, 180408 (2007).

[35] S. Takahashi, R. Hanson, J. van Tol, M. S. Sherwin, and D. D. Awschalom, Phys. Rev. Lett. **101**, 047601 (2008).

[36] A. M. Tyryshkin, S. Tojo, J. J. L. Morton, H. Riemann, N. V. Abrosimov, P. Becker, H.-J. Pohl, T. Schenkel, M. Thewalt, K. M. Itoh *et al.*, Nat. Mater. **11**, 143 (2011).

[37] C. Kutter, H. P. Moll, J. van Tol, H. Zuckermann, J. C. Maan, and P. Wyder, Phys. Rev. Lett. **74**, 2925 (1995).

[38] S. Probst, N. Kukharchyk, H. Rotzinger, A. Tkalčec, S. Wünsch, A. D. Wieck, M. Siegel, A. V. Ustinov, and P. A. Bushev, Appl. Phys. Lett. **105**, 162404 (2014).

[39] J. Klauder and P. Anderson, Phys. Rev. **125**, 912 (1962).

[40] T. Böttger, C. W. Thiel, Y. Sun, and R. L. Cone, Phys. Rev. B **73**, 075101 (2006).

[41] R. M. Brown, A. M. Tyryshkin, K. Porfyrakis, E. M. Gauger, B. W. Lovett, A. Ardavan, S. A. Lyon, G. A. D. Briggs, and J. J. L. Morton, Phys. Rev. Lett. **106**, 110504 (2011).

[42] J. H. Wesenberg, A. Ardavan, G. A. D. Briggs, J. J. L. Morton, R. J. Schoelkopf, D. I. Schuster, and K. Mølmer, Phys. Rev. Lett. **103**, 070502 (2009).

[43] H. Wu, R. E. George, J. H. Wesenberg, K. Mølmer, D. I. Schuster, R. J. Schoelkopf, K. M. Itoh, A. Ardavan, J. J. L. Morton, and G. A. D. Briggs, Phys. Rev. Lett. **105**, 140503 (2010).

[44] C. Grezes, B. Julsgaard, Y. Kubo, M. Stern, T. Umeda, J. Isoya, H. Sumiya, H. Abe, S. Onoda, T. Ohshima *et al.*, Phys. Rev. X **4**, 021049 (2014).

[45] A. J. Sigillito, H. Malissa, A. M. Tyryshkin, H. Riemann, N. V. Abrosimov, P. Becker, H.-J. Pohl, M. L. W. Thewalt, K. M. Itoh, J. J. L. Morton *et al.*, Appl. Phys. Lett. **104**, 222407 (2014).

[46] O. Benningshof, H. Mohebbi, I. Taminiau, G. Miao, and D. Cory, J. Magn. Reson. **230**, 84 (2013).

[47] C. Grezes, B. Julsgaard, Y. Kubo, W. L. Ma, M. Stern, A. Bienfait, K. Nakamura, J. Isoya, S. Onoda, T. Ohshima *et al.*, arXiv:1504.02220.

[48] E. Baldit, K. Bencheikh, P. Monnier, S. Briaudeau, J. Levenson, V. Crozatier, I. Lorgeré, F. Bretenaker, J. Le Gouët, O. Guillot-Noël *et al.*, Phys. Rev. B **81**, 144303 (2010).

[49] D. L. McAuslan, J. G. Bartholomew, M. J. Sellars, and J. J. Longdell, Phys. Rev. A **85**, 032339 (2012).

[50] G. Wolfowicz, A. M. Tyryshkin, R. E. George, H. Riemann, N. V. Abrosimov, P. Becker, H.-J. Pohl, M. L. W. Thewalt, S. A. Lyon, and J. J. L. Morton, Nat. Nanotechnol. **8**, 561 (2013).

[51] G. Wolfowicz, H. Maier-Flaig, R. Marino, A. Ferrier, H. Vezin, J. J. L. Morton, and P. Goldner, Phys. Rev. Lett. **114**, 170503 (2015).